CHAPTER IV
EFFECT OF CALCINATION TEMPERATURE ON THE PHASE TRANSITION OF NANOSIZED BARIUM TITANATE PARTICLES

4.1 Abstract

Nanosized barium titanate ($BaTiO_3$) particles were synthesized by sol-gel method. The sols were prepared by barium acetate, titanium n-butoxide, acetic acid and methanol. Thermal decomposition of the gel was studied by TG-DTA in order to seek suitable calcination temperature. In this study, the gel was calcined at different temperature varying from 600 to 1100 °C. The particle sizes and crystal structure of $BaTiO_3$ were observed by SEM and XRD, respectively. It was found that the particle size increased from nano-size to micro-size as calcination temperature increased. The crystal structure of $BaTiO_3$ transformed from cubic to tetragonal at calcination temperature of 900 °C (particle size ~ 180 nm), and tetragonality (c/a) gradually increased with increasing calcination temperature or particle size. The high tetragonal $BaTiO_3$ phase (c/a = 1.008) was obtained at calcination temperature of 1100 °C. At room temperature, the dielectric constant of $BaTiO_3$ ceramic at 1 kHz was 1230 and increased to 8320 at Curie temperature of 125 °C.

Keyword: Barium titanate, Sol-gel method, Ferroelectric, Dielectric material

4.2 Introduction

Barium titanate ($BaTiO_3$) is a well known ferroelectric material widely used in many electronic applications such as multilayer ceramic capacitor, piezoelectric transducers, pyroelectric elements and positive temperature coefficient (PTC) sensors because of its specific properties including high dielectric constant and piezoelectricity [1-3]. Recently, the tendency of the electronic industry requires miniaturization of electronic components and need to achieve higher performances in smaller structures lead to high interest in understanding the $BaTiO_3$ with nanosized

systems. Therefore, fabrication of advanced and complex electronic components requires homogeneous and pure powder with uniform and fine particle size.

Conventionally, $BaTiO_3$ powders are prepared by solid state reaction between barium carbonate ($BaCO_3$) and (TiO_2) at high temperature range of 1000-1100 °C [1], However, the $BaTiO_3$ powders obtained from the solid state reaction have some drawbacks such as large particle size with uncontrolled and irregular morphology and higher impurity due to repetitive calcinations and grinding treatments and also lower chemical reaction [4]. These drawbacks can limit the dielectric properties of the resulting sintered ceramics. In order to obtain desired properties of the $BaTiO_3$ powders, various chemical methods have been proposed for preparing fine tetragonal $BaTiO_3$ powder such as hydrothermal synthesis [5, 6], oxalate precipitation [7, 8], sol-gel method or thermal decomposition of metal alkoxide [4, 9, 10], etc. These chemical methods have potential advantages over the traditional solid state reaction method.

The $BaTiO_3$ transforms a tetragonal to a cubic phase at Curie temperature which is generally around 120-130 °C. The cubic phase shows paraelectric properties, while the tetragonal phase shows ferroelectric properties. Previously, the literature reported that $BaTiO_3$ powder synthesized at low temperature was in a cubic structure. Generally, this metastable cubic can be converted to the stable tetragonal form by calcining at high temperature (>1000 °C). Beside effect of temperature, particle size is also importance factor on phase transition [11, 12]. As particle decrease below critical particle size, it shows completely cubic phase. However, the critical particle size is different depending on synthetic method. The critical size, which the crystal changes from a tetragonal to cubic phase, had been reported in the range of 10-100 nm [13]. Yen *et al.* reported that the cubic $BaTiO_3$ powder changes to tetragonal phase, if its particle size is larger than 30 nm [14]. Xu and Gao reported that tetragonal $BaTiO_3$ prepared by hydrothermal had an average particle size of 70 nm [15]. Kwon and Yoon reported that tetragonal structure could not be observed for particle less than 170 nm. Tetragonality (*c/a*) gradually increased with increasing particle size between 170-330 and showed saturation for particle size larger than 330 nm [16]. The tetragonal $BaTiO_3$ powder has higher density, better sintering behavior,

and higher dielectric constants than cubic phase powders [17]. Therefore, changing of cubic to tetragonal phase of $BaTiO_3$ has been much interest.

The sol-gel method was used for $BaTiO_3$ synthesis in this work because of its particular advantages in obtaining fine $BaTiO_3$ powders with high chemical purity, narrow size distribution, and homogeneity through a lower temperature process, avoiding contamination of the materials. Also, it helps to maintain homogeneous mixing of two cations at molecular level [4, 18]. The aim of this study is to examine the properties of $BaTiO_3$ powder synthesized via the sol-gel method at various calcination temperatures. The transition of cubic to tetragonal was observed as functions of particle size and calcination temperature. Their dielectric properties were also measured as function of frequency and temperature.

4.3 Experimental

4.3.1 Synthesis of $BaTiO_3$ Nanocrystalline Particles

All of the chemical used for synthesis were analytical grade, and no further purification was performed before use. For preparation of sol-gel precursor gel, barium acetate [$Ba(CH_3COO)_2$, Aldrich], and titanium (iv) n-butoxide [$Ti(O(CH)_3CH_3)_4$, Aldrich] were used as starting materials. Gracial acetic acid [CH_3COOH, Labscan] and methanol [CH_3OH, Labscan] were used as solvent. The barium acetate was firstly dissolved in heat acetic acid with stirring to obtain clear solution followed by adding methanol with acetic acid: methanol ($R_{ac/me}$) of 1:2. Then the equimolar amount of titanium (iv) n-butoxide was added into this mixture under vigorous stirring. The clear solution was stable and became a gel in a few days at room temperature. The gel is formed by controlled hydrolysis and subsequent polymerization and condensation reaction to form 3-dimensional network of viscous gel. The precursor gel was converted to a dried gel by heating in vacuum oven. The dried gel was calcined by using 2-step thermal decomposition in air (Figure 4.1), in order to decompose the solvent and crystallize the barium titanate. The dried gels were calcined at different temperatures from 600-1100 °C in order to varied particle size of $BaTiO_3$ for further characterization.

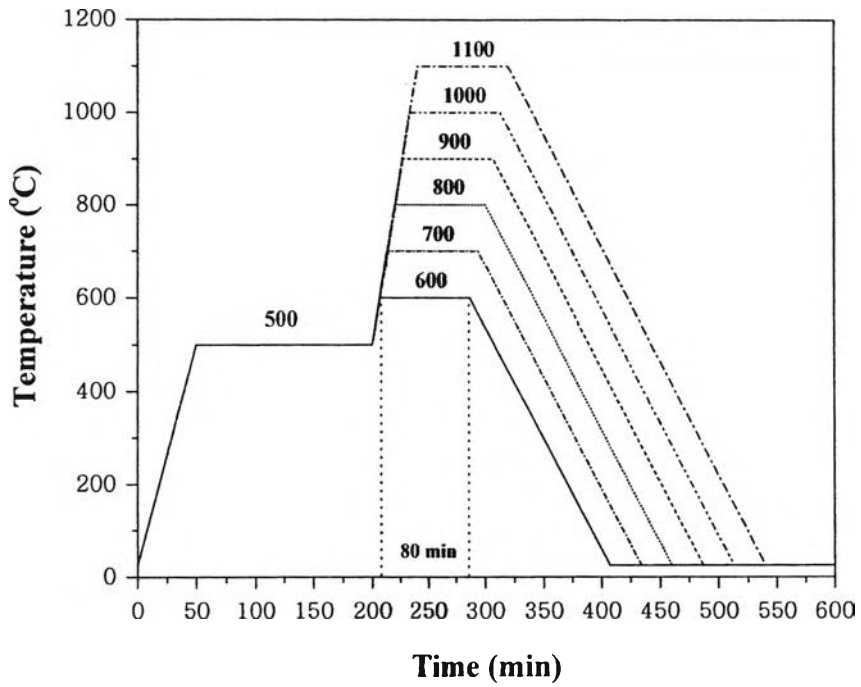

Figure 4.1 Temperature program for the 2-step thermal decomposition.

4.3.2 Preparation of $BaTiO_3$ Ceramics

The sol-gel $BaTiO_3$ powders were mixed with poly (methyl methacrylate-co-ethyl acrylate) (binder) and then press into disks shape by using a force of 10 tons for 10 mins. The sintering process was performed by putting $BaTiO_3$ pressed disks into the furnace by using the following temperature program (Figure 3.2). The temperature increases from room temperature to 300 °C with heating rate of 2.1 °C/min and hold for 2 h. Then, the temperature increases to 550 °C with the heating rate of 2.1 °C/min and hold for 5 h in order to remove binder completely. Afterward, the samples were sintered at 1350 °C for 2 h with heating rate of 4.5 °C/min from 550 °C. After sintering, the samples were cooled to room temperature at the rate of 1.7 °C/min.

4.3.3 Characterizations

Fourier-transform infrared (FT-IR) spectra of the dried and calcined $BaTiO_3$ powders were measured by fourier transformation infrared spectrophotometer (NEXUS 670 FTIR). The spectra were collected in absorbance

mode, the wave number range of 4000-400 cm^{-1} and 32 scans per resolution by the KBr pellet method.

The thermal decomposition characteristic of dried $BaTiO_3$ gel was determined by thermogravimetric-differential thermal analysis (TG-DTA, Pyris Diamond, Perkin Elmer). The dried $BaTiO_3$ gel was heated from room temperature to 1100 °C under nitrogen atmosphere with heating rate of 10 °C/min

The microstructure and morphology of $BaTiO_3$ powders and the sintered $BaTiO_3$ were investigated by using scanning electron microscope (SEM; JSM-6480LV, JEOL). The particle sizes of the $BaTiO_3$ were the average diameter of at least 20 particles from SEM micrographs. All samples were coated by gold sputtering before SEM analysis.

The diffraction patterns of $BaTiO_3$ powders were examined using X-ray diffraction (Rigaku, model Dmax 2002) with CuKα radiation and Ni-filter operated at 40 kV and 30 mA. XRD patterns were taken in the continuous mode in the 2θ range of 5-90° with the scan speed of 5 min^{-1} and sampling step of 0.02. Lattice parameters (*a* and *c*) were calculated by using the equation given below:

Cubic phase:
$$\sin^2\theta_{(hkl)} = \frac{\lambda^2(h^2+k^2+l^2)}{4a^2} \tag{4.1}$$

Tetragonal phase:
$$\sin^2\theta_{(hkl)} = \frac{\lambda^2(h^2+k^2)}{4a^2} + \frac{\lambda^2(l^2)}{4c^2} \tag{4.2}$$

For the sample preparation for dielectric measurement the sintered $BaTiO_3$ specimen were polished by SiC in order to obtain flat and parallel surfaces. The deviation in thickness affects to the experimental error in dielectric measurement. The sintered specimens were electroded by coating gold on both surfaces. The dielectric properties were measured using Hewlett-Packard 4194A impedance/gain phase analyzer. The measurements were performed at in frequency range of 1 kHz – 10 MHz and temperature range of -60-180 °C. The dielectric constant was calculated from the capacitance by using the following equation:

$$K = \frac{CA}{\varepsilon_0 d} \tag{4.3}$$

where C is the capacitance (F), ε_0 the free space dielectric constant value (8.85×10^{-12} F/m), A the capacitor area (m^2), and d the thickness of specimens.

4.4 Results and Discussion

4.4.1 Properties of Sol –Gel Barium Titanate Powders

The thermal decomposition of $BaTiO_3$ dried gel, which was prepared by sol-gel method, was investigated by TG-DTA in order to seek suitable calcination temperature of the $BaTiO_3$. TG and DTA measurement of dried gel were investigated in nitrogen atmosphere in temperature range of 30-1100 °C, as shown in Figure 4.2. The TG curve clearly shows the decomposition temperature of dried gel in two steps. The first step was a weight loss of 23.0 wt% in the temperature range of 200-500 °C, which could be attributed to the decomposition of organic compounds and species formed during the gelation process (e.g. $BaCO_3$ and/or Ba, Ti oxycarbonate). The second step was a weight loss of 7.8 wt% in the temperature range of 500-800 °C. A weak endothermic was found around 700°C corresponding $BaTiO_3$ crystallization. The small weight loss after $BaTiO_3$ crystallization occurred due to decomposition of a residual carbonate phase [19]. No weight loss was observed in the temperature more than 950 °C because the residual carbonate was possible completely decomposed. The crystallization process of $BaTiO_3$ probably occurred via the decomposition of intermediate oxycarbonate (Ba, $Ti_{oxycarbonate}$ is $Ba_2TiO_2CO_3$) as follow: [10]

$$\text{Ba, Ti}_{gel} + \text{air} \rightarrow \text{Ba, Ti}_{oxycarbonate} + CO_2$$

$$\text{Ba, Ti}_{oxycarbonate} \rightarrow 2BaTiO_3 + CO_2$$

FTIR spectra of dried gel are shown in Figure 4.3. It shows characteristic peaks due to acetate asymmetric stretching at 1566 cm^{-1} and acetate symmetric stretching at 1418 cm^{-1}, which may correspond to unreacted barium acetate and acetic acid starting materials. The 1022 cm^{-1} peak was assigned to be due to C-H bending [19]. The broad band at 3417 cm^{-1} was attributed to O-H stretching, which was disappearing at calcination temperature of 600 °C. The band at 660 cm^{-1} was assigned to Ti-O-Ti bond. Also, the band at 473 cm^{-1} corresponded to O-Ti-O bending vibration of a TiO_6 octahedron in the crystalline $BaTiO_3$ powders, but the band in wave number of 600-480 cm^{-1} related to Ti-O stretching vibration was difficult to observe due to the overlapping of adjacent bands [20].

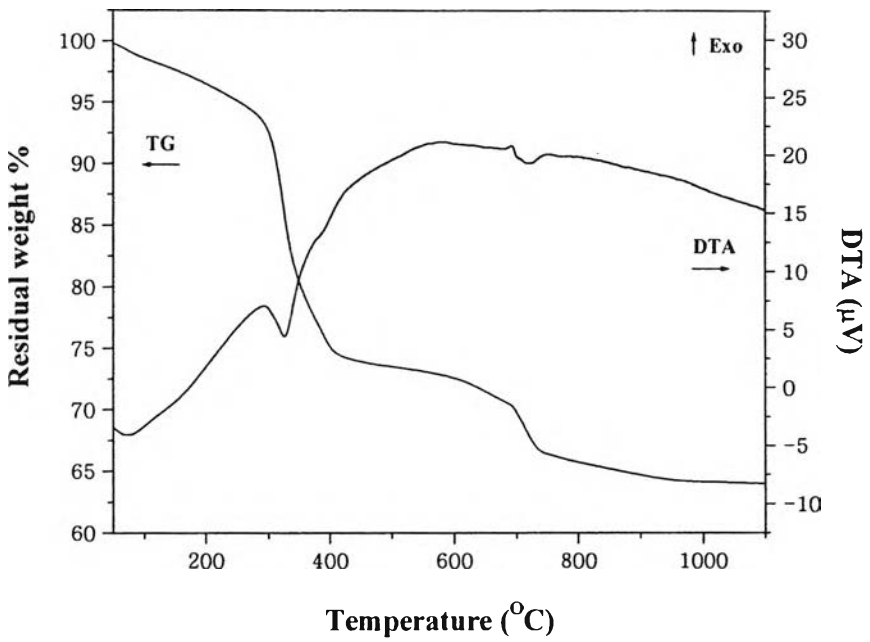

Figure 4.2 TG-DTA curve of the $BaTiO_3$ dried gel operated in nitrogen atmosphere with heating rate of 10 °C/min.

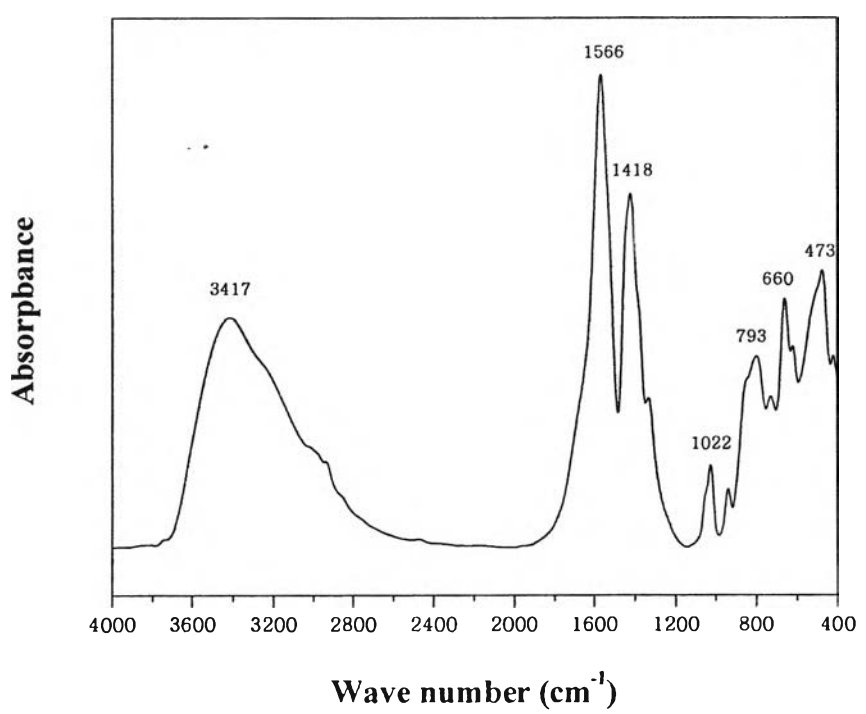

Figure 4.3 FTIR spectrum for the dried gel.

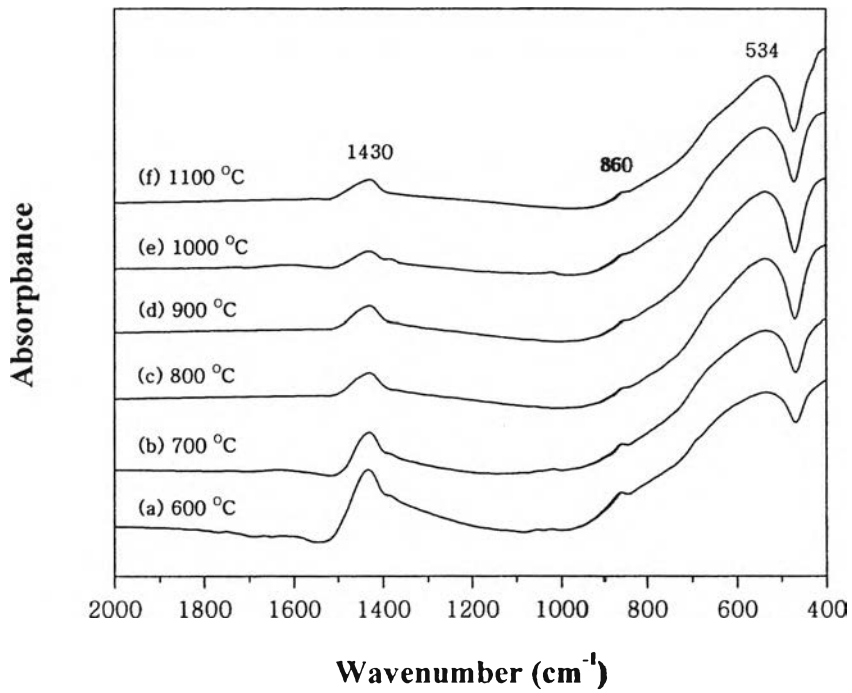

Figure 4.4 FTIR spectra for $BaTiO_3$ calcined at 600-1100 °C.

Figure 4.4 shows FTIR spectra of $BaTiO_3$ powders calcined at different temperatures. When the dried gel was calcined at 600 °C, the acetate peaks and O-H stretching disappeared, and evidence of carbonate groups appeared, as seen from peaks at 1430 cm^{-1} and 860 cm^{-1}, for C=O stretching of CO^{2-}_3 and out of plane deformation of CO^{2-}_3, respectively [19]. These peaks decreased in intensity with increasing calcinations temperature. The 534 cm^{-1}, which could not be observed in dried gel, was clearly seen due to Ti-O stretching vibration of a TiO_6 octahedron and gradually increased in intensity with increasing calcinations temperature. From these results, it was indicated that small amount of carbonate group still remain in structure after calcination at 1100 °C.

4.4.2 Effect of Calcination Temperature on Microstructure

To investigate the morphology (particle size, shape and agglomeration) of sol-gel $BaTiO_3$ powder, SEM micrographs were used to observe, as shown in Figure 4.5. The shape of sol-gel $BaTiO_3$ particles calcined at 800 °C was irregular shape. The average size of particles estimated from SEM micrographs was around 50-80 nm in diameter. The particle size and shape distribution was nearly uniform and particles were mostly agglomerated. For the $BaTiO_3$ powder calcined at

1100 °C, it can be easily observed exaggerated particle growth with the development of interparticle necks resulting in particle fusion to form larger particle (~1 μm). From this result, it could be concluded that the particle size of sol-gel $BaTiO_3$ powders increased from nano-size (88 nm at 800 °C) to micro-size (0.9 μm at 1100 °C) with increasing calcination temperature. The average particle sizes of $BaTiO_3$ calcined at different temperatures are listed in Table 4.1.

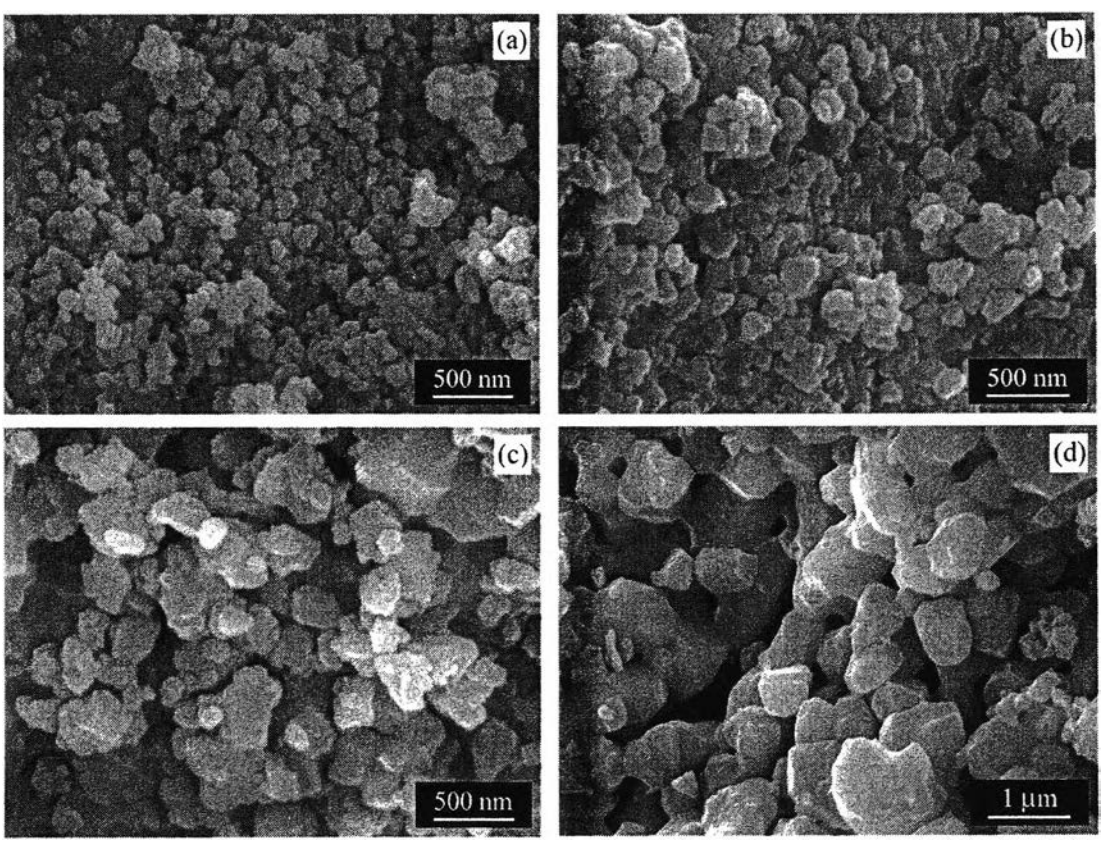

Figure 4.5 SEM micrographs of sol-gel $BaTiO_3$ powders calcined at; (a) 800 °C, (b) 900 °C, (c) 1000 °C, and 1100 °C.

Table 4.1 The average particle size of $BaTiO_3$ at different calcination temperatures

Calcination Temperature (°C)	Particle size (nm)
800	88
900	182
1000	406
1100	918

4.4.3 Effect of Calcination Temperature on Crystal Structure

To confirm the single phase of $BaTiO_3$, X-ray diffraction was used to investigate. Figure 4.6 shows XRD patterns of dried gel and $BaTiO_3$ powders calcined at different calcinations temperatures from 600 to 1100 °C. It can be seen that no peaks were observed for dried gel precursor. At the temperature of 600 °C, there were diffraction peaks of perovskite $BaTiO_3$ and $BaCO_3$ (at 2θ = 23.8, 34.2 and 42.1°). The undesirable phase ($BaCO_3$) was a regular feature of acetic synthesis. Beside the peak of $BaTiO_3$ and $BaCO_3$, there was diffraction peaks at 2θ = 26.7° corresponding to the intermediate oxycarbonate ($Ba_2Ti_2O_5CO_3$) [19]. Above this temperature, $BaTiO_3$ began to be well crystallized and the intermediate oxycarbonate disappeared. However, the peak of $BaCO_3$ was detected. It means that the decomposition of the intermediate oxycarbonate had occurred when temperature increased to 700 °C corresponding to TG-DTA result. The XRD patterns of $BaTiO_3$ calcined at 700, 800 and 900 °C show some weak peaks, corresponding to the residual carbonate phase. These peaks of residual carbonate gradually decreased in intensity as calcination temperature increased and disappear at 1000 °C, which agree with no weight loss observed after 950 °C in TG result. So a pattern of single phase $BaTiO_3$ (perovskite structure) was obtained at the calcination temperature of 1000 °C.

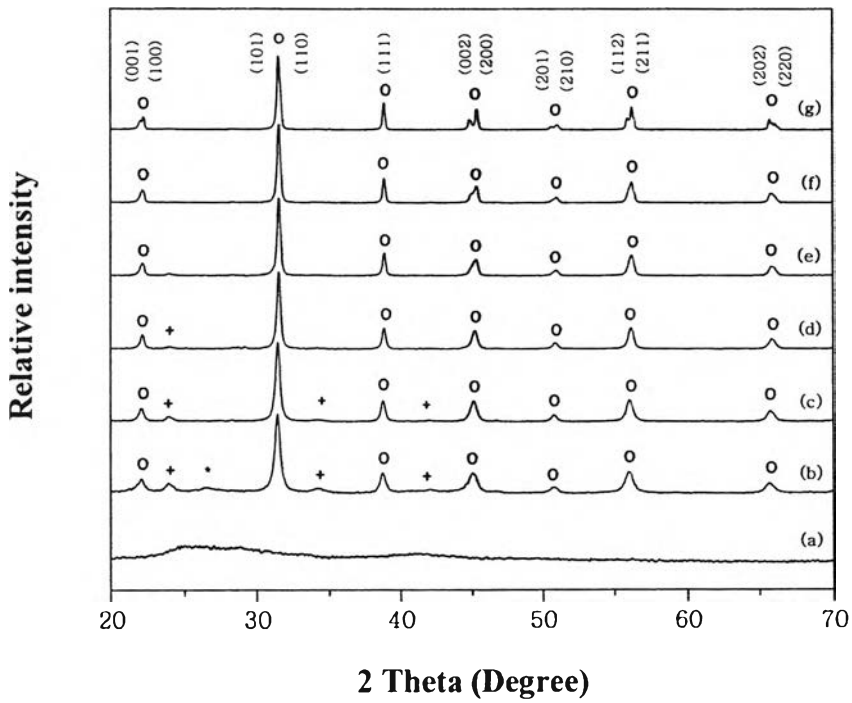

Figure 4.6 XRD patterns for dried gel and $BaTiO_3$ calcined at 600-1100 °C for 80 min: (a) dried gel, (b) 600 °C, (c) 700 °C, (d) 800 °C, (e) 900 °C, (f) 1000 °C, (g) 1100 °C (Note: ○ = $BaTiO_3$, + = $BaCO_3$, and * = $Ba_2Ti_2O_5CO_3$).

To investigate the cubic-tetragonal transition and crystal structure of the $BaTiO_3$, the most common technique is XRD. The changing of crystal structure of $BaTiO_3$ from metastable cubic to tetragonal can be identified by the peak splitting of (200)/(002) at ($2\theta \approx 45°$) [21, 22, 23]. The splitting of reflections in this region was a result of the distortion of the unit cell and the characteristic of tetragonal-$BaTiO_3$. The XRD diffraction peaks of $BaTiO_3$ in relation to calcination temperature are shown in Figure 4.7. It can be observed that no splitting of $2\theta \approx 45°$ [(002) and (200)] at the calcination temperature of 600 to 800 °C. When the calcination temperature increased to 900 °C (Figure 4.6d), the diffraction peak began to split. It refers that the crystal structure of $BaTiO_3$ was changed from metastable cubic to tetragonal. This splitting in this region was a result of the distortion of the unit cell. The splitting of the (200)/(002) gradually increased, meaning tetragonality (*c/a* ratio) was progressively enhanced with increasing calcination temperature or particle size (grain size) [24]. The slightly shift of XRD peak position to higher 2θ value with

increasing calcination temperature indicated a decrease of the lattice parameter. The lattice parameters of the $BaTiO_3$ unit cell in cubic and tetragonal phase were calculated from equation (4.1) and (4.2), respectively. As increasing calcination temperature, the lattice parameter, *a*, axis reduced while *c* axis increased, which is in agreement with report in literature [9]. The phase of the $BaTiO_3$ changed from cubic to tetragonal at 900 °C corresponding to $BaTiO_3$ particle size of 182 nm. The lattice parameters (*a* and *c*) and tetragonality (*c/a*) as a function of calcination temperature are shown in Figure 4.8 and Figure 4.9, respectively and all data are summarized in Table 4.2.

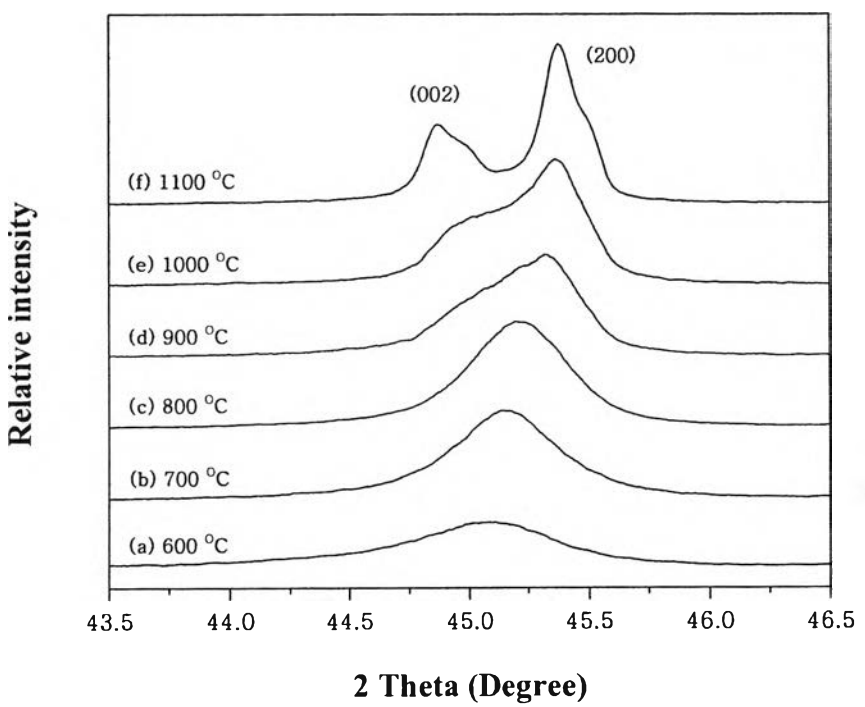

Figure 4.7 XRD patterns of sol-gel $BaTiO_3$ powders at $2\Theta \approx 45.0$ with respect to calcination temperature.

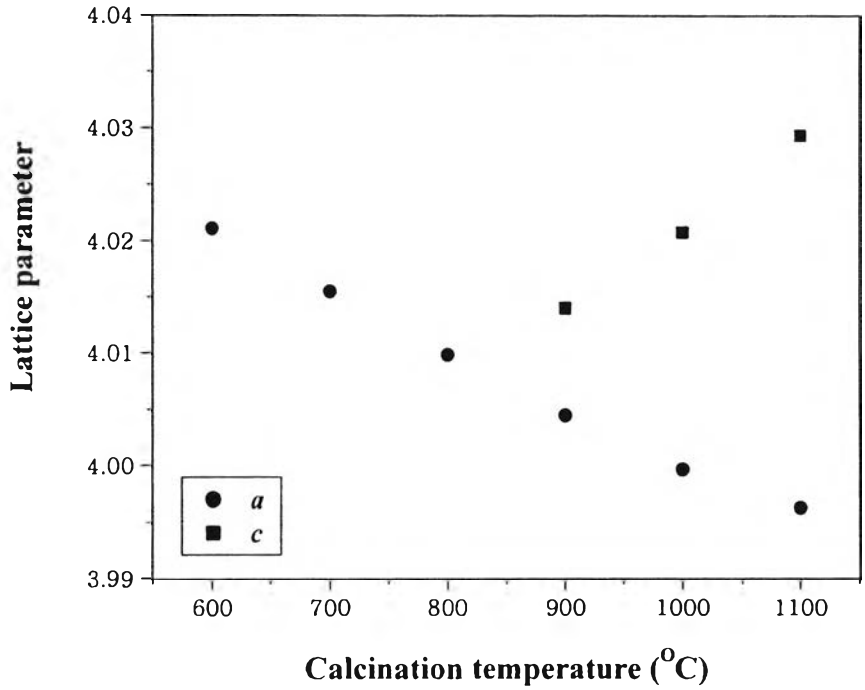

Figure 4.8 Lattice parameters (*a* and *c*) of sol-gel $BaTiO_3$ powders at different calcination temperatures.

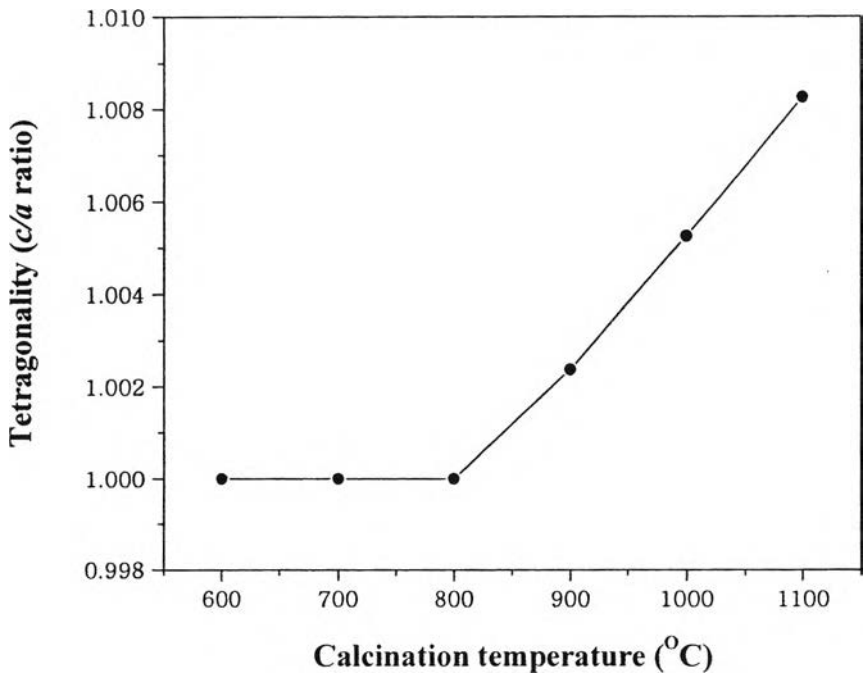

Figure 4.9 Tetragonality (*c/a* ratio) of sol-gel $BaTiO_3$ powders at different calcination temperatures.

Table 4.2 Lattice parameters, tetragonality and structure of $BaTiO_3$ calcined at different temperatures

Calcination temperature (°C)	Lattice parameter (Å)		Tetragonality	Structure
	a	*c*		
600	4.0211	-	1	Cubic
700	4.0155	-	1	Cubic
800	4.0099	-	1	Cubic
900	4.0045	4.0140	1.0024	Tetragonal
1000	3.9997	4.0207	1.0053	Tetragonal
1100	3.9963	4.0293	1.0083	Tetragonal

4.4.4 Dielectric Measurements

Sol-gel $BaTiO_3$ powders calcined at 800 °C were pressed and sintered at 1350 °C for 2 h in order to prepare $BaTiO_3$ ceramic. The dielectric constant of $BaTiO_3$ ceramic was measured in the frequency ranging from 100 Hz to 10 MHz at room temperature. As seen from Figure 4.10, the dielectric constant was found to be 1230 at 1 kHz, and loss tangent is less than 0.05. However, the dielectric constant decreased rapidly and a sudden increase in loss tangent was observed at frequency above 1 MHz. It indicated that ceramic exhibits large dielectric relaxation at frequency greater than 1 MHz (dipolar relaxation). The decrease in the dielectric constant was due to the delay in molecular polarization with respect to a changing frequency in $BaTiO_3$ ceramic.

The temperature dependence of the dielectric constant is shown in Figure 4.11. It was found that the maximum value of the dielectric constant is 8230 at temperature of 125 °C, which is defined as Curie temperature (T_C) of $BaTiO_3$ or tetragonal-cubic phase transition (T-C). This result is in agreement with previous reports. Deb *et al.* reported that T_C of pure $BaTiO_3$ was 128 °C [25]. Kinoshita and Yamaji prepared $BaTiO_3$ with various grain sizes ranging from 1 to 53 mm and found that T_C value were slightly influenced by grain size and ranged from 120 to 122 °C [26]. T_C was independent with changing frequency. Beside this transition, it

could be observed the shoulder peak corresponding to tetragonal-orthorhombic transition (T-O) at temperature of 5 °C.

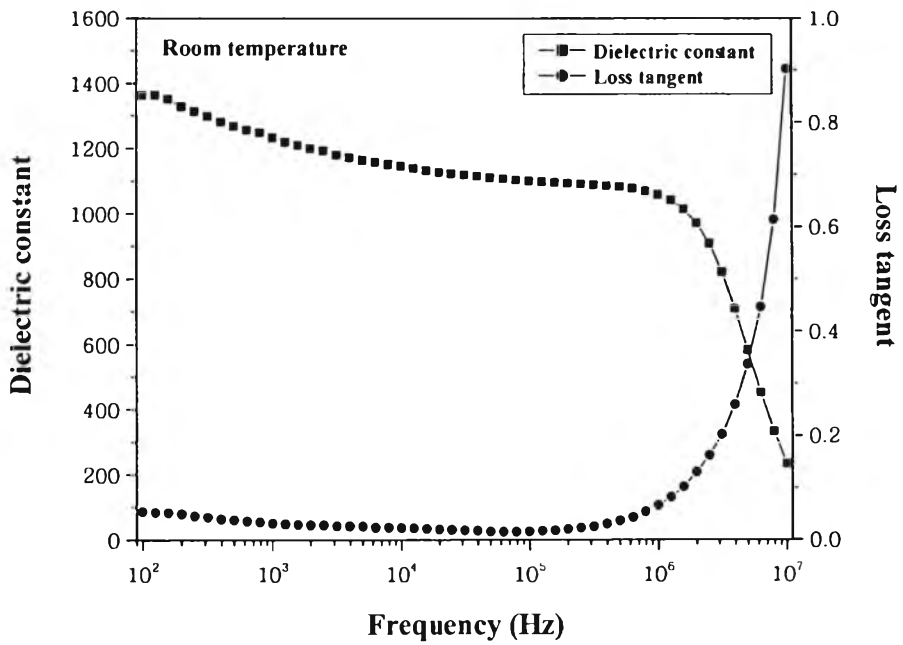

Figure 4.10 Dielectric properties as function of frequencies for $BaTiO_3$

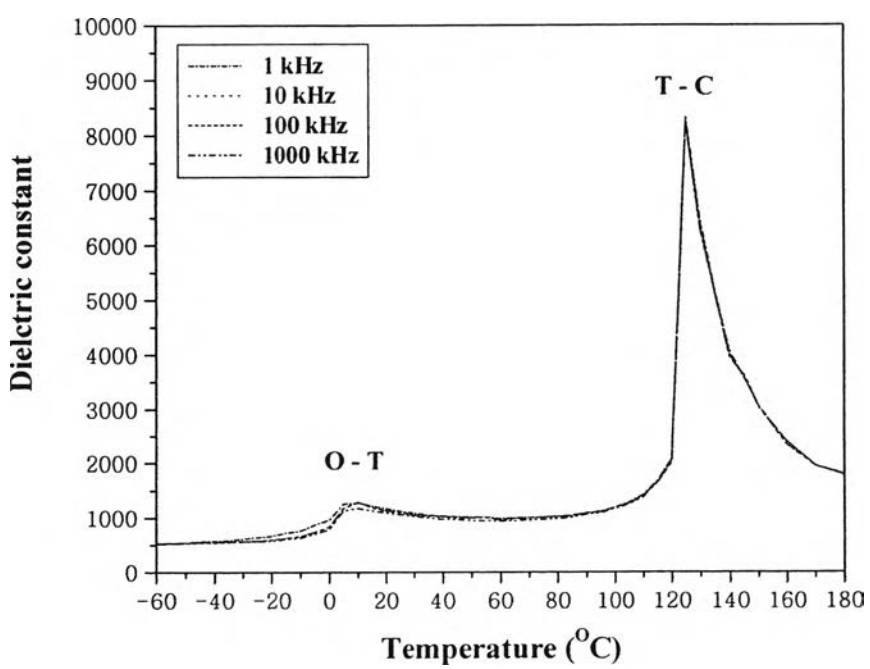

Figure 4.11 Dielectric constant as function of temperatures for $BaTiO_3$

4.5 Conclusions

From TG-DTA result, it was found that $BaTiO_3$ began to crystallize at temperature 700 °C approximately. However, some residual carbonates remain in structure at this temperature. To obtain the single phase of $BaTiO_3$, the optimum calcination temperature should be at least 800 °C. The average particle size of sol-gel $BaTiO_3$ powders calcined at 800 °C was about 88 nm with aggregation of fine particles and increased to larger particle as calcination temperature increased. At calcination temperature of 900°C, the cubic $BaTiO_3$ powders with particle size of 182 nm transformed to tetragonal phase, which was identified by the splitting at $2\theta \approx 45°$ [(200)/(002)]. The tetragonality (*c/a*) gradually increased with increasing calcination temperature or particle size. The dielectric constant of the $BaTiO_3$ ceramic showed relaxation at high frequency (> 1 MHz). The dielectric constant at room temperature was found to be 1230 and increased to maximum value (~8320) at Curie temperature (125°C).

4.6 Acknowledgements

The authors wish to thank research grants from Petroleum and Petrochemical College; the National Excellence Center for Petroleum, Petrochemical, and Advanced Materials, Thailand and the Government Research Budget Year 2005-2006

4.7 References

[1] R.C. Buchanan, Ceramic Materials for Electronic. New York: Marcel Dekker, 2004.

[2] S.L. Swartz, "Topic in electro ceramics," *IEEE Transaction on Electrical Insulation*, vol. 25(5), pp. 935-987, 1990.

[3] H.I. Won, H.H. Nersisyan, and C.W. Won, "Low temperature solid-phase synthesis of tetragonal $BaTiO_3$ powders and its characterization," *Materials Letters*, vol. 61(7), pp. 1492-1496, 2006.

[4] S.B. Deshpande, P.D. Godbole, Y.B. Khollam, and H.S. Potdar, "Characterization of barium titanate: $BaTiO_3$ (BT) ceramics prepared from sol-gel derived BT powders," *Journal of Electroceramics*, vol 15, pp. 103-108, 2005.

[5] H. Kumazawa, H.M. Cho, and E. Sada "Hydrothermal synthesis of barium titanate fine particle from amorphous and crystalline titania," *Journal of Materials Science*, vol. 30(18), pp. 4740-4744. 1995.

[6] M.H. Um and H. Kumazawa, "Hydrothermal synthesis of ferroelectric barium and strontium titanate extremely fine particle," *Journal of Material Science*, vol 35, pp. 1295-1300, 2000.

[7] S. Kim, M. Lee, T. Noh, and C. Lee, "Preparation of barium titanate by homogeneous precipitation," *Journal of Materials Science*, vol. 31, pp. 3643-3645. 2004.

[8] S. Tunkasiri and G. Rujijinakul, "Characterization of barium titanate prepared by precipitation technique," *Journal of Materials Science*, vol. 13(3), pp. 1573-4811. 2004.

[9] M.H. Frey and D.A. Payne, "Grain-size effect on structure and transformation of barium titanate," *Physical Review B*, vol. 54(5), pp. 3158-3168. 1996.

[10] A. Kareiva, S. Tautkus, R. Rapalaviciute, J. E. Jorgensen, and B. Lundtoft, "Sol-gel synthesis and characterization of barium titanate powders," *Journal of Materials Science*, vol. 34, pp. 4853-4857, 1999.

[11] K. Uchino, K. Sadanaga, T. Hirose, "Dependence of the crystal structure on particle in barium titanate," *Journal of the American Ceramic Society*, vol. 72(8), pp. 1555-1558, 1989.

[12] B.D. Begg, E.R. Vance, and J. Nowotny, "Effect of particle size on the room temperature crystal structure of barium titanate," *Journal of the American Ceramic Society*, vol. 77(12), pp. 3186-3192, 1994.

[13] T. Yan, Z.G. Shen, W.W. Zhang, and J.F. Chen, "Size dependence on the ferroelectric transition of nanosized $BaTiO_3$ particles," *Materials Chemistry and Physics*, vol. 98, pp. 450-455, 2006.

[14] F.S. Yen and H.I. Hsiang , "Fabrication and characterization of (Ba, Sr)TiO_3 thin films by sol-gel technique through organic precursor route," *Japan Journal of Applied Physics*, vol. 34, pp. 6149-6155. 1995.

[15] H. Xu and L. Gao, "Tetragoanl nanocrystalline barium titanate powder: preparation, characterization, and dielectric properties," *Journal of the American ceramic Society*, vol. 86(1), pp. 203-205. 2003.

[16] S.W. Kwon and D.H. Yoon, "Tetragonality of nano-sized barium titanate powder added with growth inhibitor upon heat treatment," *Journal of the European ceramic Society*, vol. 21(1), pp. 247-252. 2006.

[17] W. Zhu, S.A. Akbar, R. Asiaie, and P.K. Dutta, "Sintering and dielectric properties of hydrothermally synthesized cubic and tetragonal $BaTiO_3$," *Japanese Journal of Applied Physics*, vol. 36, pp. 214-221. 1997.

[18] W. Yang, A. Chang, and B. Yang, "Preparation of barium strontium titanate ceramic by sol-gel method and microwave sintering," *Journal of Materials Synthesis and Processing*, vol. 10 (6), pp. 303-309, 2003.

[19] S. Tangwiwat and S. J. Milne, "Barium titanate sols prepared by a diol-based sol-gel route," *Journal of Non-Crystalline Solids*, vol. 351, pp. 976-980, 2005.

[20] U.Y. Hwang, H.S. Park, and K.K. Koo, "Low-temperature synthesis of fully crystallized spherical $BaTiO_3$ particles by the gel-sol method," *Journal of the American Ceramic Society*, vol. 87(12), pp. 2168-2174, 2004.

[21] R.N. Viswanath and S. Ramasamy, "Preparation and ferroelectric phase transition studies of nanocrystalline $BaTiO_3$," *Nano Stuctured Materials*, vol. 8(2), pp. 155-162, 1997.

[22] R. Asiaie, W. Zhu, S. A. Akbar, and P.K. Dutta, "Characterization of submicron particles of tetragonal $BaTiO_3$," *Chemistry Materials*, vol. 8, pp. 226-234, 1996.

[23] J.M. Hwu, W.H. Yu, W.C. Yang, Y.W. Chen, and Y.Y. Chou, "Characterization of dielectric barium titanate powders prepared by homogeneous precipitation chemical reaction for embedded capacitor application," *Material Research Bulletin*, vol. 40, pp. 1662-1679, 2005.

[24] V. Buscaglia, M.T. Buscaglia, M. Viviani, L. Mitoseriu, P. Nanni, V. Trefiletti, P. Piaggio, I. Gregora, T. Ostapchuk, J. Pokorny, and J. Petzelt, "Grain size and grain boundary-related effects on the properties of nanocrystalline barium

titanate ceramic," *Journal of the European Ceramic Society*, vol. 26(14), pp. 2889-2898, 2006.

[25] K.K. Deb, M.D. Hill and J.F. Kelly, "Pyroelectric characteristics of modified barium titanate ceramics," *Journal of Material Research*, vol. 7(12), pp. 3296-3305. 1992.

[26] J.W. Liou and B.S. Chiou, "Effect of direct-current biasing on the dielectric properties of barium strontium titanate," *Journal of the American Ceramic Society*, vol. 80(12), pp. 3093-3099, 1997.